

VRMDiff: Text-Guided Video Referring Matting Generation of Diffusion

Lehan Yang¹ Jincen Song² Tianlong Wang¹
 Daiqing Qi¹ Weili Shi¹ Yuheng Liu³ Sheng Li¹

¹University of Virginia ²Columbia University ³Texas A&M University

Abstract

We propose a new task, video referring matting, which obtains the alpha matte of a specified instance by inputting a referring caption. We treat the dense prediction task of matting as video generation, leveraging the text-to-video alignment prior of video diffusion models to generate alpha mattes that are temporally coherent and closely related to the corresponding semantic instances. Moreover, we propose a new Latent-Constructive loss to further distinguish different instances, enabling more controllable interactive matting. Additionally, we introduce a large-scale video referring matting dataset with 10,000 videos. To the best of our knowledge, this is the first dataset that concurrently contains captions, videos, and instance-level alpha mattes. Extensive experiments demonstrate the effectiveness of our method. The dataset and code are available at <https://github.com/Hansxsourse/VRMDiff>.

1. Introduction

Video matting is the process of extracting precise foreground object boundaries from video sequences, widely used in video editing, film production, and augmented reality. Compared to video segmentation [7, 15, 17, 52, 67, 93], matting provides transparency information, better capturing edges and the effects of lighting. Previous video matting techniques [57, 62, 81, 100] typically focus on extracting the foreground without distinguishing between different instances. Recently, some works have differentiated between instances but cannot provide their semantic labels [35, 50], while they rely on the guidance of masks. Although these methods achieve impressive results, their scalability and usability are limited, especially in scenes involving multiple objects or when specific objects need to be designated.

Referring image matting [48, 51] has emerged as a potential solution to these limitations, utilizing natural language expressions to specify target objects in images. This approach allows for intuitive selection of target objects without needing post-adjusting, enhancing flexibility and

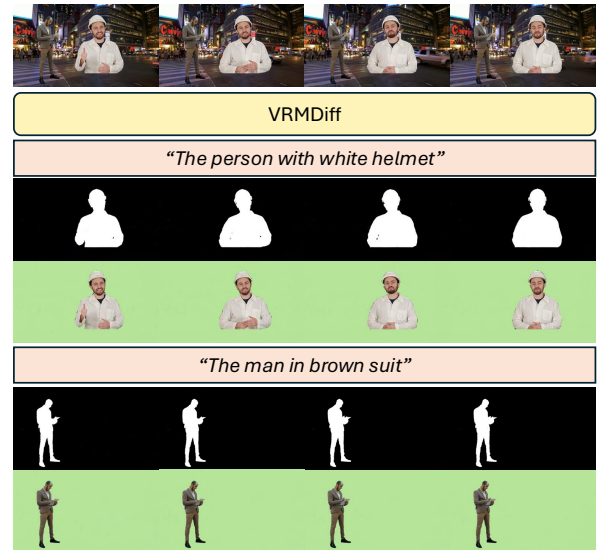


Figure 1. **Visualization results of referring matting method VRMDiff.** We treat video matting as a generation task with referring capabilities. By inputting a caption that describes the instance, our model outputs the corresponding instance’s matte.

user experience. However, extending referring image matting to videos presents significant challenges. Videos contain temporal dynamics, object motion, and complex interactions between multiple objects, requiring models capable of understanding spatiotemporal information and maintaining temporal consistency across frames. Directly applying image referring matting methods to videos lacks temporal information, making it challenging to maintain the consistency of the same instance across different frames.

Basically, in video referring matting, given a video and a caption describing an instance, we aim to output the matte corresponding to that instance specified. This task not only requires understanding the semantic content of videos and referring expressions but also dealing with issues such as object occlusion, changing lighting conditions, and overlapping objects over time. Moreover, existing video mat-

ting datasets are limited in number and do not simultaneously provide captions, videos, and instance-level mattes, which obstructs the development of data-driven approaches for this problem.

In this paper, we introduce Video Referring Matting, a new task that combines the challenges of video matting and referring expression comprehension. To facilitate research in this field, we propose VRM-10K, the first large-scale dataset for video referring matting. VRM-10K contains 10,000 videos, each with up to five foreground objects composited onto dynamic backgrounds. Each object is associated with a high-quality alpha matte and descriptive captions generated using the Tarsier [80] model, enabling fine-grained and natural language based object referencing.

To address the challenges and limitations in video referring matting outlined earlier, we propose a diffusion-based framework that effectively handles temporal dynamics and instance differentiation in videos. Diffusion models have demonstrated remarkable performance in image [13, 63, 64, 68, 83, 94] and video generation [9, 9, 28, 38, 60, 90, 98] tasks, as well as in multitask settings beyond RGB images and videos [26, 39, 61, 66, 74]. Building on these advancements, our model extends the standard diffusion process by integrating video conditional inputs and referring expressions. This integration enables the generation of accurate and temporally consistent alpha mattes based on both visual and textual information, without relying on mask guidance. Our approach effectively addresses the difficulties in maintaining temporal consistency and correctly interpreting referring expressions in videos with complex dynamics and multiple overlapping objects. Moreover, the introduction of our comprehensive VRM-10K dataset facilitates the training of such models, enabling them to learn from a rich set of annotated videos and natural language descriptions.

One key challenge in our task is handling overlapping objects and ensuring that the model correctly interprets referring expressions to isolate the target object. To address this issue, we introduce a novel latent contrastive learning approach. Specifically, we design a Latent-InfoNCE loss function that operates in the latent space of a 3D variational autoencoder. This loss encourages the model to produce latent representations close to the ground truth of the correct object while pushing away representations of incorrect or overlapping objects. This strategy effectively mitigates ambiguity and enhances the model’s ability to distinguish multiple objects based on referring expressions.

Our main contributions are summarized as follows:

- Introduction of a new task and dataset: We define the video referring matting task and construct VRM-10K dataset, a comprehensive dataset containing 10,000 videos, each with high-quality alpha mattes and corresponding natural language captions for each object.
- Diffusion-based matting framework: We develop a video

diffusion model that integrates video conditional inputs and referring expressions, without relying on mask guidance.

- Latent contrastive learning: We propose a latent contrastive loss to enhance the model’s ability to distinguish different objects in complex scenes, improving matting accuracy in multi-object and overlapping scenarios.
- Extensive experimental validation: We conduct thorough experiments to demonstrate the effectiveness of our method, showing significant improvements in matting quality and temporal coherence compared to baselines.

We believe our work lays the foundation for future research in video referring matting and opens up new possibilities for advanced applications in video processing and video understanding.

2. Related Work

Image and Video Matting. Image matting is a technique used to extract foreground objects from images by estimating their transparency, known as the alpha matte. Traditional image matting methods can be broadly categorized into two approaches: color sampling-based methods and alpha propagation-based methods. Color sampling-based methods [1, 4, 19, 24, 30] leverage low-level features to differentiate the transition areas between the foreground and background, relying on the local smoothness assumption of image statistics. However, color sampling-based methods can suffer from the problem of matte discontinuities. To address this issue, propagation-based approaches [1, 10, 27, 44, 77] aim to achieve optimal alpha values in unknown regions by leveraging the affinities of neighboring pixels. Recently, deep learning methods [16, 44, 46, 73, 85, 89, 91, 99] utilize the neural network to estimate the alpha matte with different forms of auxiliary inputs such as trimaps [8, 54, 89], sparse scribbles [44], background images [56], coarse maps [92] and mask guidance [58, 92]. In recent work, Referring Image Matting (RIM) [48] has been proposed to extract the alpha matte of a specific object based on the provided textual descriptions. Matting Anything Model [51] adopt Segment Anything Model [42] to perform the image matting.

In video matting, the accuracy of alpha matte estimation in a video sequence can be improved by exploiting the temporal context. Early works [3, 18, 45] in video matting merely extended image matting techniques to the temporal dimension but often resulted in unsatisfactory performance. Similar to image matting, trimaps are also utilized in trimap-based video matting methods [34, 72, 78, 95] to facilitate the fusion and alignment of temporal features through spatio-temporal feature aggregation. Apart from trimap-based methods, another line of works [40, 55–57, 71] adopt trimap-free approach to predict alpha mattes for the remaining video sequences. Recently, some stud-

ies [14, 47, 49, 55] have explored the use of attention mechanisms in video matting, achieving performance comparable to that of traditional CNN-based methods. Furthermore, to achieve high-quality results in video matting, Video Instance Matting [35, 50] has been proposed to extract alpha mattes for individual instances separately.

Diffusion Models for Generation. The diffusion model [68] receive numerous attentions from the research community and extensive works [20, 21, 59, 70] has been proposed to generate high-resolution images with text supervision by diffusion models. In recent years, substantial efforts have been devoted to video synthesis using diffusion models. Some early works [22, 31, 32, 41, 86] extend the text-to-image (T2I) models to synthesize the videos. One potential solution [6, 25, 53, 76] is to modify the original T2I models by incorporating additional temporal modules and training the new models on video datasets. Apart from the text-to-video generation, some works [28, 33, 82] also explore the synthesis of the videos from the images. For instance, AnimateDiff [28] generates videos by applying weighted mixing of image latents and random noise during the denoising process. However, these methods can't preserve the inherent temporal consistency in the video. To alleviate the heavy computational cost of training, some studies [65, 75, 96] have explored training-free methods for video generation. However, these training-free methods struggle to effectively preserve cross-frame consistency in textures and other details. To achieve fine-grained control over the details of synthesized videos, such as texture and motion patterns, some works [23, 82, 84, 87] leverage additional signals, such as depth or sketches, to guide the video generation process.

Diffusion for Dense Prediction. Due to the remarkable success of diffusion models in generation tasks, there is a growing interest in incorporating the generative models into dense prediction tasks, such as depth estimation and semantic segmentation. Recently, some works [2, 11, 12, 26, 66, 74, 79] attempted to perform the visual perception tasks using the diffusion models. These works [5, 88, 97] either reuse or merge latent features of U-Nets [69] to perform segmentation and depth estimation tasks. Additionally, some efforts have been made to bridge the gap between the generation tasks and the dense prediction tasks. Lee et.al. [43] leveraged the the pretrained text-to-image models as a prior and proposed an image-to-prediction diffusion process to adapt the text-to-image models for the dense prediction problems. He et.al. [29] proposed a task switcher to preserve the fine-grained details during dense annotation generation. Other approaches [5, 36, 37] accomplish the same goal by formulating the dense prediction tasks as visual-condition-guided generation processes.

3. Method

3.1. Video Referring Matting

3.1.1. Problem Definition

Task	Instance	Text-guid
Video Matting	✗	✗
Video Instance Matting	✓	✗
Video Referring Matting	✓	✓

Table 1. Comparison between video referring matting and related video matting task.

Unlike video matting and video instance matting, as shown in Table 1, our task not only distinguishes different instances but also uses captions as guidance to specify the object to be matted. We consider a video sequence $I \in \mathbb{R}^{T \times H \times W \times 3}$ consists of T frames, where each frame I_t , with $t \in \{1, \dots, T\}$, has spatial dimensions $H \times W$. Given a natural language prompt P that describes a target object in the video, the goal of video referring matting task is to generate a temporally consistent alpha matte $\alpha_t^i(P)$ that accurately isolates the described object while preserving fine-grained details such as transparency and soft boundaries. Unlike conventional video matting approaches, our model dynamically interprets both visual and textual information to infer precise object boundaries directly from the given prompt and video.

To achieve this process, our model learns to predict an alpha matte for each video frame, capturing fine-grained transparency and soft object boundaries while maintaining temporal consistency. Given a background image B_t and a foreground layer F_t , the observed video frame can be formulated as:

$$I_t = \alpha_t(P) \circ F_t + (1 - \alpha_t(P)) \circ B_t, \quad (1)$$

where $\alpha_t(P) \in [0, 1]^{H \times W \times 1}$ represents the alpha matte of the target object in frame t , conditioned on the prompt P , ensuring that only the described region contributes to the final matte. The foreground layer $F_t \in \mathbb{R}^{H \times W \times 3}$ represents the region of interest extracted from the input video, while $B_t \in \mathbb{R}^{H \times W \times 3}$ represents the background. The operator \circ denotes the Hadamard product, enforcing per-element blending of the foreground and background.

Our approach utilizes a diffusion-based framework CogVideoX [90] to iteratively refine the predicted alpha matte, ensuring spatial precision and temporal consistency. By conditioning the diffusion process on both the input video and the prompt, the model progressively denoises latent representations to generate high-quality mattes. This formulation allows the model to generalize across diverse objects, varying backgrounds, and complex motion pat-

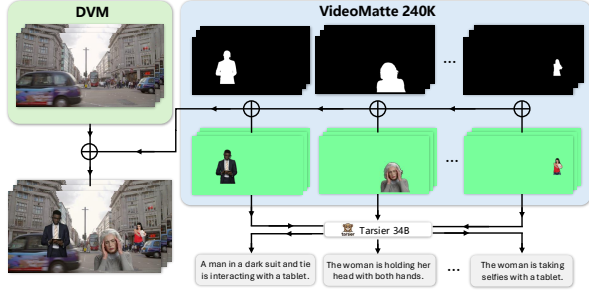


Figure 2. **Data pipeline.** For the background videos, we sample from DVM, and for the foreground instances, we sample from VideoMatte240K. The foreground instances are composited onto the background videos. The instance-level captions are generated by the vision-language model Tarsier, using the matte-extracted instance videos as input.

terms, making it well-suited for flexible and scalable video editing applications.

3.1.2. Dataset

Compared to image matting, video matting lacks sufficient datasets to support the training of diffusion models. Therefore, as the data pipeline shown in Figure 2, we propose VRM-10K, a multi-instance video matting dataset with high-quality alpha mattes and corresponding captions for each instance, totaling 10K videos of 120 frames each. Since the foregrounds in VideoMatte240K [56] do not include the original backgrounds, we sample background videos from DVM [78] and foreground instances from VideoMatte240K. Specifically, we set the maximum number of foreground instances per video to five. For each randomly sampled background video, we determine the number of foreground instances to include by sampling from a normal distribution ranging from one to five. We then randomly select that number of foreground instances from VideoMatte240K. Each foreground instance is resized, repositioned, and applied onto the background video, the corresponding alpha matte undergoes the same transformation during this step. Moreover, we limit the size differences among foreground instances within the same video to prevent significant disparities. For the text captions, we use the 34B Tarsier [80], inputting the foreground instance videos to generate descriptive and diverse captions.

3.2. Diffusion Method

In our video referring matting framework shown in Figure 3, diffusion models serve as the core mechanism for refining predicted alpha mattes by progressively denoising a latent representation of the input video frames. The model begins with an initial noisy estimate and iteratively removes noise, ensuring the generated alpha mattes maintain both high fidelity and temporal consistency across frames.

To formalize this process, we define a forward diffusion

model that gradually corrupts the original clean video frame x_0 by adding Gaussian noise at each step. The corrupted latent representation at time step t , denoted as x_t , follows the distribution:

$$q(x_t|x_0) = \mathcal{N}(\sqrt{\bar{\alpha}_t}x_0, (1 - \bar{\alpha}_t)I), \quad (2)$$

where $q(x_t|x_0)$ represents the probability distribution of x_t given the clean frame x_0 . The term $\bar{\alpha}_t$ is a variance schedule that determines the amount of noise added at step t , gradually increasing as t progresses. The identity matrix I ensures that the noise introduced at each step follows an isotropic Gaussian distribution.

To recover the clean video frame x_0 , the reverse process aims to iteratively remove noise from x_t by predicting an intermediate latent representation at each step. The probability distribution of the denoised frame at step $t - 1$, given x_t , is formulated as:

$$p_\theta(x_{t-1}|x_t) = \mathcal{N}(\mu_\theta(x_t, t), \sigma_t^2 I), \quad (3)$$

where $p_\theta(x_{t-1}|x_t)$ represents the probability distribution of the denoised latent state x_{t-1} given the current noisy state x_t . The term $\mu_\theta(x_t, t)$ is a function that predicts the mean of this distribution, parameterized by θ , which represents the learnable weights of the denoising model. The variance σ_t^2 controls the uncertainty of the prediction at each step.

By progressively refining x_t , the model is able to recover high-quality alpha mattes that align with the textual prompt while ensuring smooth transitions between video frames.

3.2.1. Video-Conditioned Diffusion

Unlike standard diffusion-based video generation models CogVideoX [90], where the diffusion process is guided solely by text prompts and temporal dependencies, our framework introduces an additional video-conditioned input. This enables the model to leverage both spatiotemporal coherence from the reference video and the generative capabilities of diffusion models. Specifically, we expand the input channel dimension from 16 to 32 to accommodate the additional video signal.

Given an input reference video x_t^{video} , we encode it using a 3D Variational Autoencoder (3D VAE) to obtain its latent representation z_t^{video} . Similarly, a pure Gaussian noise sample x_t^{noise} is encoded using the same 3D VAE, producing z_t^{noise} . These two latent representations are then concatenated to form the input for the diffusion transformer:

$$z_t = \text{Concat}(z_t^{\text{video}}, z_t^{\text{noise}}), \quad (4)$$

where z_t represents the latent representation at time step t , composed of: z_t^{video} , the latent embedding obtained from the encoded reference video. z_t^{noise} , the latent representation of the noise injected during the forward diffusion process.

This concatenated latent representation is then fed into the diffusion transformer, allowing the model to maintain

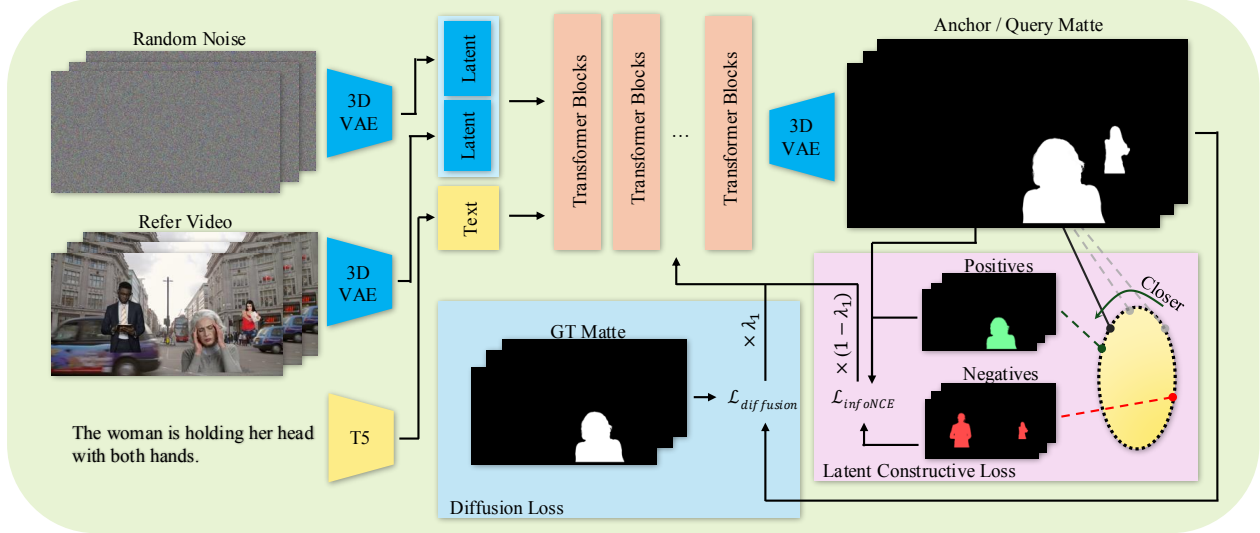


Figure 3. **Overview of VRMDiff framework.** Similar to CogVideoX, our method performs denoising in the latent space using a 3D VAE. We input the conditional video and the corresponding referring caption, and the model is expected to output the alpha matte decoded into RGB space by the 3D VAE. Besides the diffusion loss, we employ a latent contrastive loss. During training, we use the model’s latent output as the anchor, the ground truth matte as the positive sample, and instance mattes not corresponding to the caption as negative samples. This approach enhances the model’s ability to distinguish instances and improves text-to-instance alignment.

temporal consistency across frames while benefiting from the generative flexibility of the diffusion process.

3.2.2. Text-Conditioned Matte Generation

Beyond video conditioning, our model incorporates textual guidance to enhance the semantic alignment between the generated matte and the user-provided prompt. Instead of dynamically injecting text information at each transformer block, we encode the textual description once and integrate it into the initial input representation. Given an input prompt T , we obtain its dense embedding using a T5 encoder:

$$e_{\text{text}} = \text{T5-Encoder}(T). \quad (5)$$

The diffusion transformer then receives a combination of the video-conditioned latent representation and the text embedding as input:

$$h_0 = \text{TransformerInput}(z_t, e_{\text{text}}), \quad (6)$$

where h_0 is the initial feature embedding. The term z_t represents the concatenated latent representation of the video-conditioned embedding and the noise input.

Once injected into the transformer, the feature representation is iteratively refined through multiple layers. The updated representation at layer l is given by: $h_l = \text{TransformerBlock}(h_{l-1})$ where h_l denotes the feature representation at layer l of the diffusion transformer.

3.3. Latent Contrastive Learning

Referring matting presents a fundamental challenge: different objects in the scene may share similar visual features,

making it difficult to differentiate the correct foreground object based solely on visual cues. Our goal is to ensure that the predicted matte aligns with the reference description while maintaining separation between ambiguous objects. To achieve this, we leverage contrastive learning in the latent space, encouraging the model to generate mattes that are not only structurally accurate but also well-aligned with the text prompt.

A direct approach to training the model would be to minimize the pixel-wise L2 loss:

$$\mathcal{L}_{\text{pixel}} = \|M - \hat{M}\|^2. \quad (7)$$

However, this approach fails to capture high-level object semantics and struggles with ambiguous cases where multiple objects share similar textures. To explicitly enforce separation in the latent space, we assume that the predicted matte embedding \hat{z} should be closer to the true matte embedding z than to incorrect matte embeddings. This motivates the use of contrastive learning, where we minimize the distance between positive pairs while pushing negative samples apart:

$$\mathcal{L}_{\text{InfoNCE}} = -\log \frac{\exp(\text{sim}(\hat{z}, z^+)/\tau)}{\sum_{z^-} \exp(\text{sim}(\hat{z}, z^-)/\tau)}, \quad (8)$$

where $z^+ = \text{VAE}(M)$ is the ground truth matte embedding, z^- represents negative samples, i.e., incorrect matte embeddings, $\text{sim}(a, b)$ is the cosine similarity function:

$$\text{sim}(a, b) = \frac{a \cdot b}{\|a\| \|b\|}, \quad (9)$$

and τ is a temperature scaling parameter.

While contrastive learning in pixel space is possible, it is computationally inefficient and fails to capture object-level relationships. Instead, we perform contrastive learning in the latent space by leveraging the 3D VAE, which achieves an $8 \times 8 \times 4$ compression from pixels to latent representations, thereby significantly reducing computational complexity. In our framework, we define $p(z)$ as the ground truth latent distribution obtained by encoding the ground truth matte M via the VAE (i.e., $p(z) = \text{VAE}(M)$), and $q(\hat{z})$ as the predicted latent distribution obtained from the predicted matte \hat{M} (i.e., $q(\hat{z}) = \text{VAE}(\hat{M})$). To quantify the discrepancy between these distributions, we consider the Kullback-Leibler (KL) divergence:

$$D_{\text{KL}}(q(\hat{z})||p(z)) = \int q(\hat{z}) \log \frac{q(\hat{z})}{p(z)} d\hat{z},$$

which measures how well the predicted latent distribution $q(\hat{z})$ approximates the ground truth distribution $p(z)$. This formulation encourages the model to generate latent representations that align closely with the semantics of the ground truth matte while filtering out high-frequency noise. Then, using pixel space representations results in sparsely distributed embeddings, making KL divergence estimation unreliable. Formally, the variance of the KL estimate can be written as:

$$\text{Var}(D_{\text{KL}}) = \mathbb{E}[(\log q(\hat{z}) - \log p(z))^2] - D_{\text{KL}}^2. \quad (10)$$

Since pixel space embeddings are high-dimensional and sparse, the expectation term grows large, leading to an unstable estimation of D_{KL} . In contrast, by mapping the input to a structured latent space, we obtain a more compact distribution, improving the stability of contrastive learning.

Another advantage of working in the latent space is its ability to absorb minor misalignments, increasing the tolerance to small prediction errors. Let $M \in \mathbb{R}^{H \times W}$ denote the ground truth alpha matte, representing the per-pixel opacity of the target object, where $M(i, j) \in [0, 1]$ at each spatial location (i, j) . Suppose the predicted matte \hat{M} contains minor noise ϵ in pixel space:

$$\hat{M} = M + \epsilon. \quad (11)$$

Applying the VAE encoder to the noisy matte produces the corresponding latent representation:

$$\hat{z} = \text{VAE}(M + \epsilon). \quad (12)$$

If the VAE is trained to minimize reconstruction loss, then the expected reconstruction error satisfies:

$$\mathbb{E}\|\text{VAE}^{-1}(z) - M\|^2 \leq \lambda\|\epsilon\|^2, \quad (13)$$

where λ is a compression factor determined by the VAE architecture. Since $\lambda < 1$ in a well-trained VAE, the transformation effectively suppresses high-frequency noise, leading

	MAD (\downarrow)	MSE (\downarrow)	Grad (\downarrow)	Conn (\uparrow)
Baseline	0.0875	0.0831	0.0012	0.9137
VRMDiff	0.0689	0.0668	0.0014	0.9293

Table 2. **Evaluation of distance metrics for referring matting.** MAD, MSE, Grad and Conn stand for mean absolute differences, mean squared error, gradient and connectivity respectively.

	RQ (\uparrow)	TQ (\uparrow)	MQ (\uparrow)	VIMQ (\uparrow)
Baseline	16.18	38.31	33.75	2.09
VRMDiff	37.00	74.59	49.66	13.71

Table 3. **Evaluation of matting quality metrics for referring matting.** RQ, TQ, MQ and VIMQ stand for recognition quality, tracking quality, instance-level matting quality and video instance-aware matting quality respectively.

to a more robust matte representation. Consequently, small spatial errors in pixel space have a reduced impact in the latent space, resulting in more stable and temporally consistent matte predictions.

To jointly optimize matte reconstruction and feature separation, we define the final loss function:

$$\mathcal{L} = \lambda_1 \mathcal{L}_{\text{diffusion}} + (1 - \lambda_1) \mathcal{L}_{\text{InfoNCE}}. \quad (14)$$

where $\mathcal{L}_{\text{diffusion}} = \mathbb{E}\|\epsilon - \epsilon_\theta(z_t, t)\|^2$ is the standard diffusion loss, and $\mathcal{L}_{\text{InfoNCE}}$ ensures feature separation in latent space.

By applying contrastive learning in the latent space, our model improves the robustness of matte generation, achieving better alignment between textual descriptions and object-level representations.

4. Experiments

In this section, we first evaluate our method’s performance on the new video referring matting task using datasets involving multiple objects, and then compare it with previous instance and caption agnostic video matting methods. We use basic metrics such as MAD, MSE, Gradient, and Connectivity for general measurements, and also employ metrics focused on instance matting [50], including Matting Quality (MQ), Tracking Quality (TQ), Recognition Quality (RQ), and their product, Video Instance-aware Matting Quality (VIMQ), to better assess the quality of matting and the alignment between the referring condition and the generated results. In the ablation study, we investigate the capability of InfoNCE in latent space for contrastive learning, verifying the effectiveness of Latent InfoNCE.

4.1. Experimental Settings

We conduct our experiments using the VRM-10K dataset synthesized from DVM and VideoMatte240K. This dataset



Figure 4. **Single instance matting qualitative results on VRMDiff.** Six frames are evenly sampled from the video, with the horizontal axis representing time and the frame index gradually increasing. From top to bottom, the sequence is the input video, the output alpha matte, and the extracted instance obtained by applying the matte to the video. The prompts are *A man in a dark suit and tie* and *The man is wearing a dark blue suit jacket, a white shirt, and black headphones.*

Method	Type	Backbone	MAD (\downarrow)	MSE (\downarrow)	Grad (\downarrow)	Conn (\uparrow)
RVM [57]	Instance-agnostic	MobileNet V3	0.0294	0.0258	0.0024	0.9609
RVM [57]	Instance-agnostic	ResNet 50	0.0334	0.0294	0.0024	0.9549
VRMDiff (Ours)	Referring	CogVideoX 2B	0.0689	0.0668	0.0014	0.9293

Table 4. **Comparison between instance and caption agnostic method and referring method.** MAD, MSE, Grad and Conn stand for mean absolute differences, mean squared error, gradient and connectivity respectively.

includes 9000 training samples and 1000 validation samples. The training and validation samples are independently partitioned during dataset creation, derived from entirely different splits of DVM and VideoMatte240K. We initialize our model weights with the CogVideoX 2B text-to-video model. The weights of the original input channels are re-sampled to obtain weights for the video condition channels. Our experiments are conducted on two NVIDIA A40 48G GPUs, with a batch size of 1 per GPU, fine-tuning for 10000 steps using a learning rate of $1e-5$.

4.2. Video Referring Matting

For the video referring matting task, since we are the first to propose this task, there are no prior works for direct comparison. Therefore, in our experiments, we compare our complete method with a baseline model that in-

corporates video conditioning into CogVideoX. All models are trained under the same conditions and data for the same number of steps. As shown in Table 2 and 3, our method demonstrates improvements over the video-conditioned CogVideoX across various metrics, confirming the effectiveness of our approach. Additionally, our method exhibits better text-to-matte alignment and captures more continuous and consistent motion.

We compared instance-agnostic and caption-agnostic methods. These methods can only distinguish between foreground and background, unable to differentiate among different instances, and do not use captions as conditions. For these methods, we evaluated their performance on the validation set of our VRM-10K, combining the instance matte ground truths into a single foreground matte. As shown in Table 4, our class and caption aware method per-



Figure 5. **Multiple instance matting qualitative results on VRMDiff.** Six frames are evenly sampled from the video, with the horizontal axis representing time and the frame index gradually increasing. We use masks of different colors to represent the alpha mattes of different instances.

λ	MAD (\downarrow)	MSE (\downarrow)	Grad (\downarrow)	Conn (\uparrow)
0.1	0.0689	0.0668	0.0014	0.9293
0.25	0.0754	0.0721	0.0013	0.9240
0.5	0.0886	0.0824	0.0012	0.9138

Table 5. **Ablation study on contrastive loss weight.** RQ, TQ, MQ and VIMQ stand for recognition quality, tracking quality, instance-level matting quality and video instance-aware matting quality respectively.

forms slightly lower than the class-agnostic method RVM in MAD, MSE, and Connectivity metrics but outperforms them in the Gradient metric. Although this comparison is relatively unfavorable to our method due to the more challenging task and objectives, achieving comparable performance demonstrates the effectiveness of our approach.

4.3. Qualitative Results

Figure 4 illustrates our video matting generation capability in scenarios with complex backgrounds and single foregrounds. The referring ability not only accurately locates the instance specified by the caption in complex scenes, but also enables our generated mattes to extract high quality instances without including background elements precisely. Meanwhile, in Figure 5, we present the quality of multi-object referring matting in situations with multiple foreground subjects under both simple and complex backgrounds. Our model maintains good text-to-instance alignment in these cases and performs well on both large-size and small-size objects.

λ	RQ (\uparrow)	TQ (\uparrow)	MQ (\uparrow)	VIMQ (\uparrow)
0.1	37.00	74.59	49.66	13.71
0.25	25.62	53.31	38.28	5.23
0.5	7.41	18.59	9.68	0.13

Table 6. **Ablation study on contrastive loss weight.** MAD, MSE, Grad and Conn stand for mean absolute differences, mean squared error, gradient and connectivity respectively.

4.4. Ablation Study

The primary training objective of the diffusion model remains generation. We treat the video matting task as a video generation task and use contrastive loss to regulate text-to-instance alignment. Here, we ablate the weight lambda of the contrastive loss in the total loss. The results in Table 5 and 6 show that our choice of 0.1 achieves optimal performance on the majority of metrics.

5. Conclusion

In this paper, we introduces Video Referring Matting, a novel task that aims to extract the alpha matte of target objects in videos based on natural language queries. Treating the alpha matte as an RGB video and using diffusion models for generative matting, integrates video conditional inputs and referring expressions without relying on mask guidance. We propose a latent contrastive learning approach that improves matting accuracy and temporal coherence, enhance the model’s ability to distinguish different objects in complex scenes. Additionally, we present a large-scale captioned video referring matting dataset. Extensive experiments demonstrate the effectiveness of our method, showing significant improvements over baseline approaches.

References

- [1] Yagiz Aksoy, Tunc Ozan Aydin, and Marc Pollefeys. Designing effective inter-pixel information flow for natural image matting. In *CVPR*, pages 29–37, 2017. 2
- [2] Tomer Amit, Tal Shaharbany, Eliya Nachmani, and Lior Wolf. Segdiff: Image segmentation with diffusion probabilistic models. *arXiv*, 2021. 3
- [3] Nicholas Apostoloff and Andrew Fitzgibbon. Bayesian video matting using learnt image priors. In *CVPR*, pages I–I. IEEE, 2004. 2
- [4] Xue Bai and Guillermo Sapiro. A geodesic framework for fast interactive image and video segmentation and matting. In *ICCV*, pages 1–8. IEEE, 2007. 2
- [5] Dmitry Baranchuk, Andrey Voynov, Ivan Rubachev, Valentin Khrukov, and Artem Babenko. Label-efficient semantic segmentation with diffusion models. In *ICLR*. OpenReview.net, 2022. 3
- [6] Andreas Blattmann, Robin Rombach, Huan Ling, Tim Dockhorn, Seung Wook Kim, Sanja Fidler, and Karsten Kreis. Align your latents: High-resolution video synthesis with latent diffusion models. In *CVPR*, pages 22563–22575, 2023. 3
- [7] Adam Botach, Evgenii Zheltonozhskii, and Chaim Baskin. End-to-end referring video object segmentation with multimodal transformers. In *CVPR*, pages 4985–4995, 2022. 1
- [8] Shaofan Cai, Xiaoshuai Zhang, Haoqiang Fan, Haibin Huang, Jiangyu Liu, Jiaming Liu, Jiaying Liu, Jue Wang, and Jian Sun. Disentangled image matting. In *ICCV*, pages 8819–8828, 2019. 2
- [9] Haoxin Chen, Yong Zhang, Xiaodong Cun, Menghan Xia, Xintao Wang, Chao Weng, and Ying Shan. Videocrafter2: Overcoming data limitations for high-quality video diffusion models. In *CVPR*, pages 7310–7320, 2024. 2
- [10] Qifeng Chen, Dingzeyu Li, and Chi-Keung Tang. Knn matting. *TPAMI*, 35(9):2175–2188, 2013. 2
- [11] Shoufa Chen, Peize Sun, Yibing Song, and Ping Luo. Diffusionet: Diffusion model for object detection. In *ICCV*, pages 19830–19843, 2023. 3
- [12] Ting Chen, Lala Li, Saurabh Saxena, Geoffrey Hinton, and David J Fleet. A generalist framework for panoptic segmentation of images and videos. In *ICCV*, pages 909–919, 2023. 3
- [13] Xi Chen, Lianghua Huang, Yu Liu, Yujun Shen, Deli Zhao, and Hengshuang Zhao. Anydoor: Zero-shot object-level image customization. In *CVPR*, pages 6593–6602, 2024. 2
- [14] Bowen Cheng, Ishan Misra, Alexander G Schwing, Alexander Kirillov, and Rohit Girdhar. Masked-attention mask transformer for universal image segmentation. In *Proceedings of the IEEE/CVF conference on computer vision and pattern recognition*, pages 1290–1299, 2022. 3
- [15] Ho Kei Cheng, Seoung Wug Oh, Brian Price, Alexander Schwing, and Joon-Young Lee. Tracking anything with decoupled video segmentation. In *ICCV*, pages 1316–1326, 2023. 1
- [16] Donghyeon Cho, Yu-Wing Tai, and Inso Kweon. Natural image matting using deep convolutional neural networks. In *ECCV*, pages 626–643. Springer, 2016. 2
- [17] Suhwan Cho, Minhyeok Lee, Seunghoon Lee, Dogyoon Lee, Heeseung Choi, Ig-Jae Kim, and Sangyoun Lee. Dual prototype attention for unsupervised video object segmentation. In *CVPR*, pages 19238–19247, 2024. 1
- [18] Inchang Choi, Minhaeng Lee, and Yu-Wing Tai. Video matting using multi-frame nonlocal matting laplacian. In *ECCV*, pages 540–553. Springer, 2012. 2
- [19] Yung-Yu Chuang, Brian Curless, David H Salesin, and Richard Szeliski. A bayesian approach to digital matting. In *CVPR*, pages II–II. IEEE, 2001. 2
- [20] Katherine Crowson, Stefan Andreas Baumann, Alex Birch, Tanishq Mathew Abraham, Daniel Z Kaplan, and Enrico Shippole. Scalable high-resolution pixel-space image synthesis with hourglass diffusion transformers. In *ICML*, 2024. 3
- [21] Zheng Ding, Mengqi Zhang, Jiajun Wu, and Zhuowen Tu. Patched denoising diffusion models for high-resolution image synthesis. In *ICLR*, 2023. 3
- [22] Patrick Esser, Johnathan Chiu, Parmida Atighehchian, Jonathan Granskog, and Anastasis Germanidis. Structure and content-guided video synthesis with diffusion models. In *ICCV*, pages 7312–7322. IEEE, 2023. 3
- [23] Patrick Esser, Johnathan Chiu, Parmida Atighehchian, Jonathan Granskog, and Anastasis Germanidis. Structure and content-guided video synthesis with diffusion models. In *ICCV*, pages 7346–7356, 2023. 3
- [24] Xiaoxue Feng, Xiaohui Liang, and Zili Zhang. A cluster sampling method for image matting via sparse coding. In *ECCV*, pages 204–219. Springer, 2016. 2
- [25] Songwei Ge, Seungjun Nah, Guilin Liu, Tyler Poon, Andrew Tao, Bryan Catanzaro, David Jacobs, Jia-Bin Huang, Ming-Yu Liu, and Yogesh Balaji. Preserve your own correlation: A noise prior for video diffusion models. In *ICCV*, pages 22930–22941, 2023. 3
- [26] Zigang Geng, Binxin Yang, Tiankai Hang, Chen Li, Shuyang Gu, Ting Zhang, Jianmin Bao, Zheng Zhang, Houqiang Li, Han Hu, et al. Instructdiffusion: A generalist modeling interface for vision tasks. In *CVPR*, pages 12709–12720, 2024. 2, 3
- [27] Leo Grady, Thomas Schiwietz, Shmuel Aharon, and Rüdiger Westermann. Random walks for interactive alpha-matting. In *VIP*, pages 423–429. Citeseer, 2005. 2
- [28] Yuwei Guo, Ceyuan Yang, Anyi Rao, Zhengyang Liang, Yaohui Wang, Yu Qiao, Maneesh Agrawala, Dahua Lin, and Bo Dai. Animatediff: Animate your personalized text-to-image diffusion models without specific tuning. In *ICLR*, 2024. 2, 3
- [29] Jing He, Haodong Li, Wei Yin, Yixun Liang, Leheng Li, Kaiqiang Zhou, Hongbo Zhang, Bingbing Liu, and Ying-Cong Chen. Lotus: Diffusion-based visual foundation model for high-quality dense prediction. *arXiv*, 2024. 3
- [30] Kaiming He, Christoph Rhemann, Carsten Rother, Xiaoou Tang, and Jian Sun. A global sampling method for alpha matting. In *CVPR*, pages 2049–2056. Ieee, 2011. 2

- [31] Jonathan Ho, Tim Salimans, Alexey Gritsenko, William Chan, Mohammad Norouzi, and David J Fleet. Video diffusion models. *NeurIPS*, 35:8633–8646, 2022. 3
- [32] Wenyi Hong, Ming Ding, Wendi Zheng, Xinghan Liu, and Jie Tang. Cogvideo: Large-scale pretraining for text-to-video generation via transformers. In *ICLR*. OpenReview.net, 2023. 3
- [33] Li Hu. Animate anyone: Consistent and controllable image-to-video synthesis for character animation. In *CVPR*, pages 8153–8163, 2024. 3
- [34] Wei-Lun Huang and Ming-Sui Lee. End-to-end video matting with trimap propagation. In *CVPR*, pages 14337–14347, 2023. 2
- [35] Chuong Huynh, Seoung Wug Oh, Abhinav Shrivastava, and Joon-Young Lee. Maggie: Masked guided gradual human instance matting. In *CVPR*, pages 3870–3879, 2024. 1, 3
- [36] Haorui Ji, Taojun Lin, and Hongdong Li. Dpbridge: Latent diffusion bridge for dense prediction. *arXiv*, 2024. 3
- [37] Yuanfeng Ji, Zhe Chen, Enze Xie, Lanqing Hong, Xihui Liu, Zhaoqiang Liu, Tong Lu, Zhenguo Li, and Ping Luo. Ddp: Diffusion model for dense visual prediction. In *ICCV*, pages 21741–21752, 2023. 3
- [38] Yang Jin, Zhicheng Sun, Ningyuan Li, Kun Xu, Hao Jiang, Nan Zhuang, Quzhe Huang, Yang Song, Yadong Mu, and Zhouchen Lin. Pyramidal flow matching for efficient video generative modeling. *arXiv preprint arXiv:2410.05954*, 2024. 2
- [39] Bingxin Ke, Anton Obukhov, Shengyu Huang, Nando Metzger, Rodrigo Caye Daudt, and Konrad Schindler. Repurposing diffusion-based image generators for monocular depth estimation. In *CVPR*, pages 9492–9502, 2024. 2
- [40] Zhanghan Ke, Jiayu Sun, Kaican Li, Qiong Yan, and Rynson WH Lau. Modnet: Real-time trimap-free portrait matting via objective decomposition. In *AAAI*, pages 1140–1147, 2022. 2
- [41] Levon Khachatryan, Andranik Movsisyan, Vahram Tadevosyan, Roberto Henschel, Zhangyang Wang, Shant Navasardyan, and Humphrey Shi. Text2video-zero: Text-to-image diffusion models are zero-shot video generators. In *ICCV*, pages 15954–15964, 2023. 3
- [42] Alexander Kirillov, Eric Mintun, Nikhila Ravi, Hanzi Mao, Chloe Rolland, Laura Gustafson, Tete Xiao, Spencer Whitehead, Alexander C Berg, Wan-Yen Lo, et al. Segment anything. In *ICCV*, pages 4015–4026, 2023. 2
- [43] Hsin-Ying Lee, Hung-Yu Tseng, and Ming-Hsuan Yang. Exploiting diffusion prior for generalizable dense prediction. In *CVPR*, pages 7861–7871, 2024. 3
- [44] Anat Levin, Dani Lischinski, and Yair Weiss. A closed-form solution to natural image matting. *TPAMI*, 30(2):228–242, 2007. 2
- [45] Dingzeyu Li, Qifeng Chen, and Chi-Keung Tang. Motion-aware knn laplacian for video matting. In *ICCV*, pages 3599–3606, 2013. 2
- [46] Jizhizi Li, Jing Zhang, and Dacheng Tao. Deep automatic natural image matting. *arXiv*, 2021. 2
- [47] Jiachen Li, Marianna Ohanyan, Vidit Goel, Shant Navasardyan, Yunchao Wei, and Humphrey Shi. Video-matt: A simple baseline for accessible real-time video matting. In *CVPR*, pages 2177–2186, 2023. 3
- [48] Jizhizi Li, Jing Zhang, and Dacheng Tao. Referring image matting. In *CVPR*, pages 22448–22457, 2023. 1, 2
- [49] Jiachen Li, Vidit Goel, Marianna Ohanyan, Shant Navasardyan, Yunchao Wei, and Humphrey Shi. Vm-former: End-to-end video matting with transformer. In *WACV*, pages 6678–6687, 2024. 3
- [50] Jiachen Li, Roberto Henschel, Vidit Goel, Marianna Ohanyan, Shant Navasardyan, and Humphrey Shi. Video instance matting. In *CVPR*, pages 6668–6677, 2024. 1, 3, 6
- [51] Jiachen Li, Jitesh Jain, and Humphrey Shi. Matting anything. In *CVPR*, pages 1775–1785, 2024. 1, 2
- [52] Minghan Li, Shuai Li, Xindong Zhang, and Lei Zhang. Univs: Unified and universal video segmentation with prompts as queries. In *CVPR*, pages 3227–3238, 2024. 1
- [53] Xin Li, Wenqing Chu, Ye Wu, Weihang Yuan, Fanglong Liu, Qi Zhang, Fu Li, Haocheng Feng, Errui Ding, and Jingdong Wang. Videogen: A reference-guided latent diffusion approach for high definition text-to-video generation. *arXiv*, 2023. 3
- [54] Yaoyi Li and Hongtao Lu. Natural image matting via guided contextual attention. In *AAAI*, pages 11450–11457, 2020. 2
- [55] Chung-Ching Lin, Jiang Wang, Kun Luo, Kevin Lin, Linjie Li, Lijuan Wang, and Zicheng Liu. Adaptive human matting for dynamic videos. In *CVPR*, pages 10229–10238, 2023. 2, 3
- [56] Shanchuan Lin, Andrey Ryabtsev, Soumyadip Sengupta, Brian L Curless, Steven M Seitz, and Ira Kemelmacher-Shlizerman. Real-time high-resolution background matting. In *CVPR*, pages 8762–8771, 2021. 2, 4
- [57] Shanchuan Lin, Linjie Yang, Imran Saleemi, and Soumyadip Sengupta. Robust high-resolution video matting with temporal guidance. In *WACV*, pages 238–247, 2022. 1, 2, 7
- [58] Jinlin Liu, Yuan Yao, Wendi Hou, Miaomiao Cui, Xuan-song Xie, Changshui Zhang, and Xian-sheng Hua. Boosting semantic human matting with coarse annotations. In *CVPR*, pages 8563–8572, 2020. 2
- [59] Yanzuo Lu, Manlin Zhang, Andy J Ma, Xiaohua Xie, and Jianhuang Lai. Coarse-to-fine latent diffusion for pose-guided person image synthesis. In *CVPR*, pages 6420–6429, 2024. 3
- [60] Xin Ma, Yaohui Wang, Gengyun Jia, Xinyuan Chen, Ziwei Liu, Yuan-Fang Li, Cunjian Chen, and Yu Qiao. Latte: Latent diffusion transformer for video generation. *arXiv preprint arXiv:2401.03048*, 2024. 2
- [61] Quang Nguyen, Truong Vu, Anh Tran, and Khoi Nguyen. Dataset diffusion: Diffusion-based synthetic data generation for pixel-level semantic segmentation. *NeurIPS*, 36: 76872–76892, 2023. 2
- [62] Kwanyong Park, Sanghyun Woo, Seoung Wug Oh, In So Kweon, and Joon-Young Lee. Mask-guided matting in the wild. In *CVPR*, pages 1992–2001, 2023. 1

- [63] William Peebles and Saining Xie. Scalable diffusion models with transformers. In *ICCV*, pages 4195–4205, 2023. [2](#)
- [64] Dustin Podell, Zion English, Kyle Lacey, Andreas Blattmann, Tim Dockhorn, Jonas Müller, Joe Penna, and Robin Rombach. Sdxl: Improving latent diffusion models for high-resolution image synthesis. *arXiv preprint arXiv:2307.01952*, 2023. [2](#)
- [65] Chenyang Qi, Xiaodong Cun, Yong Zhang, Chenyang Lei, Xintao Wang, Ying Shan, and Qifeng Chen. Fatezero: Fusing attentions for zero-shot text-based video editing. In *ICCV*, pages 15932–15942, 2023. [3](#)
- [66] Lu Qi, Lehan Yang, Weidong Guo, Yu Xu, Bo Du, Varun Jampani, and Ming-Hsuan Yang. Unigs: Unified representation for image generation and segmentation. In *CVPR*, pages 6305–6315, 2024. [2, 3](#)
- [67] Nikhila Ravi, Valentin Gabeur, Yuan-Ting Hu, Ronghang Hu, Chaitanya Ryal, Tengyu Ma, Haitham Khedr, Roman Rädle, Chloe Rolland, Laura Gustafson, Eric Mintun, Junting Pan, Kalyan Vasudev Alwala, Nicolas Carion, Chao-Yuan Wu, Ross Girshick, Piotr Dollar, and Christoph Feichtenhofer. SAM 2: Segment anything in images and videos. In *ICLR*, 2025. [1](#)
- [68] Robin Rombach, Andreas Blattmann, Dominik Lorenz, Patrick Esser, and Björn Ommer. High-resolution image synthesis with latent diffusion models. In *CVPR*, pages 10684–10695, 2022. [2, 3](#)
- [69] Olaf Ronneberger, Philipp Fischer, and Thomas Brox. U-net: Convolutional networks for biomedical image segmentation. In *MICCAI*, pages 234–241, 2015. [3](#)
- [70] Axel Sauer, Frederic Boesel, Tim Dockhorn, Andreas Blattmann, Patrick Esser, and Robin Rombach. Fast high-resolution image synthesis with latent adversarial diffusion distillation. In *SIGGRAPH*, pages 1–11, 2024. [3](#)
- [71] Soumyadip Sengupta, Vivek Jayaram, Brian Curless, Steven M Seitz, and Ira Kemelmacher-Shlizerman. Background matting: The world is your green screen. In *CVPR*, pages 2291–2300, 2020. [2](#)
- [72] Hongje Seong, Seoung Wug Oh, Brian Price, Euntai Kim, and Joon-Young Lee. One-trimap video matting. In *ECCV*, pages 430–448. Springer, 2022. [2](#)
- [73] Xiaoyong Shen, Xin Tao, Hongyun Gao, Chao Zhou, and Jiaya Jia. Deep automatic portrait matting. In *ECCV*, pages 92–107. Springer, 2016. [2](#)
- [74] Shelly Sheynin, Adam Polyak, Uriel Singer, Yuval Kirstain, Amit Zohar, Oron Ashual, Devi Parikh, and Yaniv Taigman. Emu edit: Precise image editing via recognition and generation tasks. In *CVPR*, pages 8871–8879, 2024. [2, 3](#)
- [75] Fengyuan Shi, Jiayi Gu, Hang Xu, Songcen Xu, Wei Zhang, and Limin Wang. Bivdiff: A training-free framework for general-purpose video synthesis via bridging image and video diffusion models. In *CVPR*, pages 7393–7402, 2024. [3](#)
- [76] Uriel Singer, Adam Polyak, Thomas Hayes, Xi Yin, Jie An, Songyang Zhang, Qiyuan Hu, Harry Yang, Oron Ashual, Oran Gafni, Devi Parikh, Sonal Gupta, and Yaniv Taigman. Make-a-video: Text-to-video generation without text-video data. In *ICLR*, 2023. [3](#)
- [77] Jian Sun, Jiaya Jia, Chi-Keung Tang, and Heung-Yeung Shum. Poisson matting. In *ACM SIGGRAPH*, pages 315–321. ACM, 2004. [2](#)
- [78] Yanan Sun, Guanzhi Wang, Qiao Gu, Chi-Keung Tang, and Yu-Wing Tai. Deep video matting via spatio-temporal alignment and aggregation. In *CVPR*, pages 6975–6984, 2021. [2, 4](#)
- [79] Chaoyang Wang, Xiangtai Li, Lu Qi, Henghui Ding, Yunhai Tong, and Ming-Hsuan Yang. Semflow: Binding semantic segmentation and image synthesis via rectified flow. *NeurIPS*, 37:138981–139001, 2024. [3](#)
- [80] Jiawei Wang, Liping Yuan, Yuchen Zhang, and Hao-miao Sun. Tarsier: Recipes for training and evaluating large video description models, 2024. *arXiv preprint arXiv:2407.00634*, 2024. [2, 4](#)
- [81] Tiantian Wang, Sifei Liu, Yapeng Tian, Kai Li, and Ming-Hsuan Yang. Video matting via consistency-regularized graph neural networks. In *ICCV*, pages 4902–4911, 2021. [1](#)
- [82] Xiang Wang, Hangjie Yuan, Shiwei Zhang, Dayou Chen, Jiuniu Wang, Yingya Zhang, Yujun Shen, Deli Zhao, and Jingren Zhou. Videocomposer: Compositional video synthesis with motion controllability. *NeurIPS*, 36:7594–7611, 2023. [3](#)
- [83] Xudong Wang, Trevor Darrell, Sai Saketh Rambhatla, Rohit Girdhar, and Ishan Misra. Instancediffusion: Instance-level control for image generation. In *CVPR*, pages 6232–6242, 2024. [2](#)
- [84] Xiang Wang, Shiwei Zhang, Hangjie Yuan, Zhiwu Qing, Biao Gong, Yingya Zhang, Yujun Shen, Changxin Gao, and Nong Sang. A recipe for scaling up text-to-video generation with text-free videos. In *CVPR*, pages 6572–6582, 2024. [3](#)
- [85] Yu Wang, Yi Niu, Peiyong Duan, Jianwei Lin, and Yuanjie Zheng. Deep propagation based image matting. In *IJCAI*, pages 999–1006, 2018. [2](#)
- [86] Jay Zhangjie Wu, Yixiao Ge, Xintao Wang, Stan Weixian Lei, Yuchao Gu, Yufei Shi, Wynne Hsu, Ying Shan, Xiaohu Qie, and Mike Zheng Shou. Tune-a-video: One-shot tuning of image diffusion models for text-to-video generation. In *ICCV*, pages 7623–7633, 2023. [3](#)
- [87] Jinbo Xing, Menghan Xia, Yuxin Liu, Yuechen Zhang, Yong Zhang, Yingqing He, Hanyuan Liu, Haoxin Chen, Xiaodong Cun, Xintao Wang, et al. Make-your-video: Customized video generation using textual and structural guidance. *TCVS*, 2024. [3](#)
- [88] Jiarui Xu, Sifei Liu, Arash Vahdat, Wonmin Byeon, Xiaolong Wang, and Shalini De Mello. Open-vocabulary panoptic segmentation with text-to-image diffusion models. In *CVPR*, pages 2955–2966, 2023. [3](#)
- [89] Ning Xu, Brian Price, Scott Cohen, and Thomas Huang. Deep image matting. In *CVPR*, pages 2970–2979, 2017. [2](#)
- [90] Zhuoyi Yang, Jiayan Teng, Wendi Zheng, Ming Ding, Shiyu Huang, Jiazheng Xu, Yuanming Yang, Wenyi Hong, Xiaohan Zhang, Guanyu Feng, Da Yin, Yuxuan Zhang, Weihang Wang, Yean Cheng, Bin Xu, Xiaotao Gu, Yuxiao Dong, and Jie Tang. Cogvideox: Text-to-video diffusion models with an expert transformer. In *ICLR*, 2025. [2, 3, 4](#)

- [91] Haichao Yu, Ning Xu, Zilong Huang, Yuqian Zhou, and Humphrey Shi. High-resolution deep image matting. In *AAAI*, pages 3217–3224, 2021. 2
- [92] Qihang Yu, Jianming Zhang, He Zhang, Yilin Wang, Zhe Lin, Ning Xu, Yutong Bai, and Alan Yuille. Mask guided matting via progressive refinement network. In *CVPR*, pages 1154–1163, 2021. 2
- [93] Linfeng Yuan, Miaojing Shi, Zijie Yue, and Qijun Chen. Losh: Long-short text joint prediction network for referring video object segmentation. In *CVPR*, pages 14001–14010, 2024. 1
- [94] Lvmin Zhang, Anyi Rao, and Maneesh Agrawala. Adding conditional control to text-to-image diffusion models. In *ICCV*, pages 3836–3847, 2023. 2
- [95] Yunke Zhang, Chi Wang, Miaomiao Cui, Peiran Ren, Xuansong Xie, Xian-Sheng Hua, Hujun Bao, Qixing Huang, and Weiwei Xu. Attention-guided temporally coherent video object matting. In *ACM MM*, pages 5128–5137, 2021. 2
- [96] Yabo Zhang, Yuxiang Wei, Dongsheng Jiang, Xiaopeng Zhang, Wangmeng Zuo, and Qi Tian. Controlvideo: Training-free controllable text-to-video generation. In *ICLR*. OpenReview.net, 2024. 3
- [97] Wenliang Zhao, Yongming Rao, Zuyan Liu, Benlin Liu, Jie Zhou, and Jiwen Lu. Unleashing text-to-image diffusion models for visual perception. In *ICCV*, pages 5729–5739, 2023. 3
- [98] Yupeng Zhou, Daquan Zhou, Ming-Ming Cheng, Jiashi Feng, and Qibin Hou. Storydiffusion: Consistent self-attention for long-range image and video generation. *NeurIPS*, 37:110315–110340, 2025. 2
- [99] Bingke Zhu, Yingying Chen, Jinqiao Wang, Si Liu, Bo Zhang, and Ming Tang. Fast deep matting for portrait animation on mobile phone. In *ACM MM*, pages 297–305, 2017. 2
- [100] Dongqing Zou, Xiaowu Chen, Guangying Cao, and Xiaogang Wang. Video matting via sparse and low-rank representation. In *ICCV*, pages 1564–1572, 2015. 1

A. Appendix

This supplementary material provides additional visualization results, details about the VRM-10K video referring matting dataset. The contents of this supplementary material are organized as follows:

- VRM-10K Dataset details.
- Additional visualization results, including examples of video referring matting.

Additionally, please see the mp4 file in our supplementary material to view the *recorded video* that provides a concise overview of our paper.

B. VRM-10K Dataset Details

We have recorded that in the 9,000 samples of the training set in our VRM-10K dataset, the mean number of instances

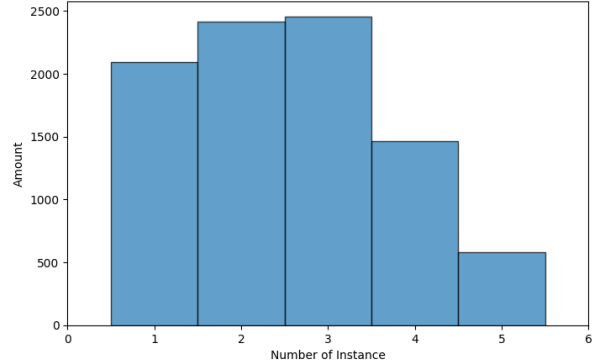


Figure 6. **Distribution of instance number in the video referring matting dataset.** The X-axis represents the groups of the total number of instances in a single video, while the Y-axis represents the total number of videos appearing in this group.

is 2.5581 with a standard deviation of 1.1926. The overall distribution is shown in Figure 6.

C. More Visualization Results

We provide additional visualizations in Figures 7 and 8. In various scenarios with both simple and complex backgrounds, our referring matting method consistently achieves precise alpha mattes.

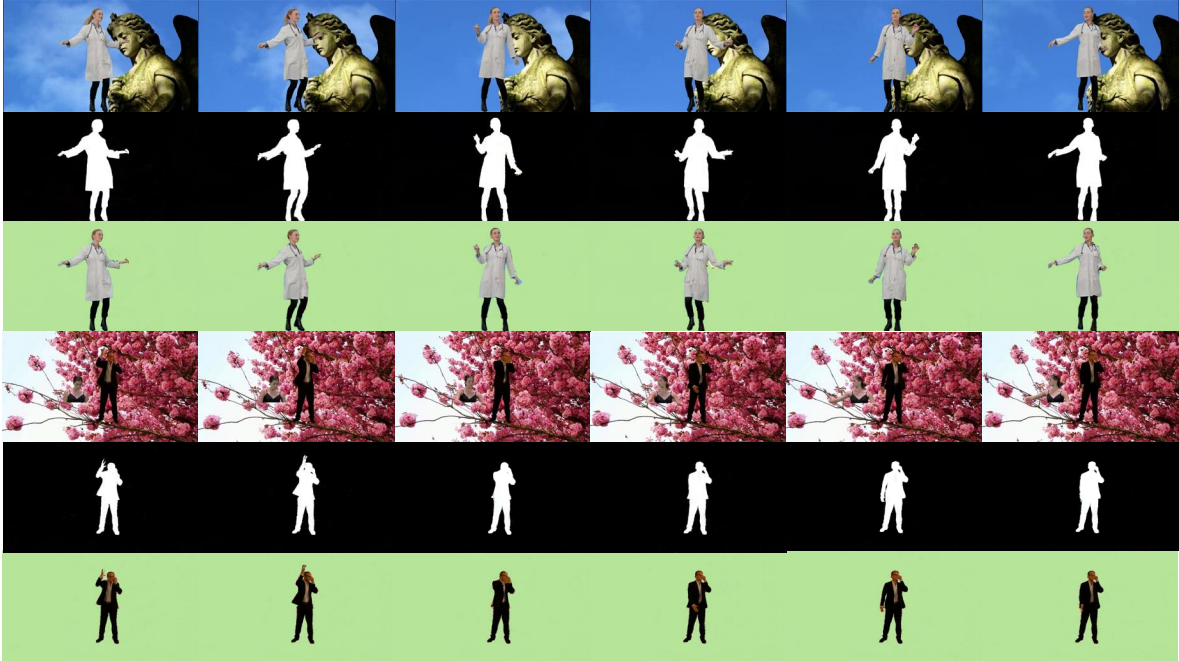


Figure 7. **More examples on referring video matting quality.** Six frames are evenly sampled from the video, with the horizontal axis representing time and the frame index gradually increasing. From top to bottom, the sequence is the input video, the output alpha matte, and the extracted instance obtained by applying the matte to the video.

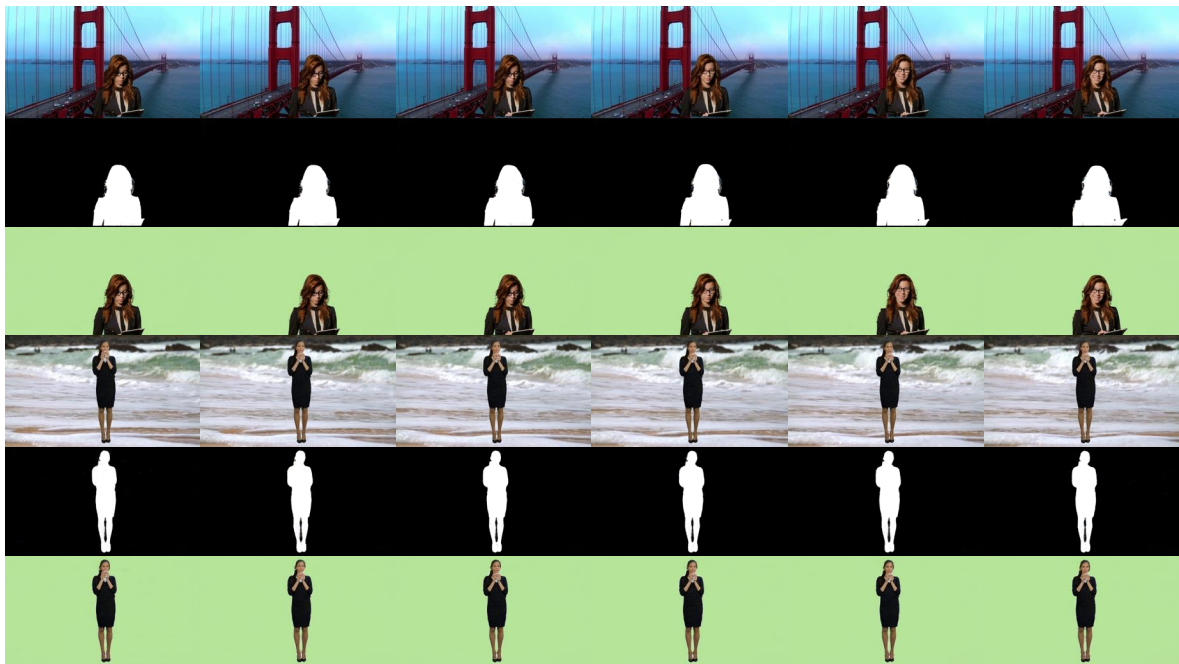


Figure 8. **More examples on referring video matting quality.** Six frames are evenly sampled from the video, with the horizontal axis representing time and the frame index gradually increasing. From top to bottom, the sequence is the input video, the output alpha matte, and the extracted instance obtained by applying the matte to the video.